Bulletin of the Mineral Research and Exploration

http://bulletin.mta.gov.tr

Mineralogical and geochemical characterization of Thanetian-Ypresian Phosphatic Layers in the Djemi-Djema Deposit

Salim BOULEMIA[a-b], Riheb HADJI[c-d], Fares AMARA[e], Rahal ABID[e] and Younes HAMED[f]

[a] *Faculty of Natural and Life Sciences Earth and the Universe, University May 8, 1945, Guelma, BP 401 Guelma 24000 - Algeria.*
[b] *Laboratory of Sedimentary Environment and Hydric and Minerals Resources. Echahid Larbi Tebessi University, route de constantine, 12002, Tebessa, Algeria.*
[c] *Department of Earth Sciences, Institute of Architecture and Earth Sciences, Farhat Abbas University, El Bez campus. Setif 19137, Algeria.*
[d] *Laboratory of Applied Research in Engineering Geology, Geotechnics, Water Sciences, and Environment, Farhat Abbas University, El Bez campus. Setif 19137, Algeria.*
[e] *SOMIPHOS Company, P3R7+VRR, Bir El Ater, ZHUN II BP 122, Tébessa, Algeria.*
[f] *Laboratory for the Application of Materials to the Environment, Water and Energy (LAM3E), Faculty of Science of Gafsa, University of Gafsa, Route de Tozeur - 2112 Gafsa, Tunisia.*

Research Article

Keywords:
X-Ray Diffraction, Apatite Minerals, Geochemical Data, Lithological Succession, Spatial Irregularities.

ABSTRACT

The Jebel El Onk region presents a complex geological history, starting with Maastrichtian limestones. Early Paleocene subsidence intensified, leading to the deposition of thick marly horizons and black marl shales during the early Thanetian. This was followed by the formation of a significant phosphate sequence during the late Thanetian to early Ypresian, comprising interbedded marls, phosphorites, and dolomites, and concluding with lagoonal gypsum marls and phosphate-rich clays, subsequently overlain by Miocene sediments. This study focuses on the Jebel-Onk phosphate deposit, with a particular emphasis on characterizing diverse phosphate facies and assessing their implications for resource management. Using X-ray Diffraction analysis, the apatite group minerals and associated rock components from the Djemi-Djema-East deposit were identified. To further elucidate the deposit's morphology and surrounding lithology, the study integrated geochemical data and lithological succession derived from core drilling. An automatic mapping of the Paleo-Eocene stratiform phosphate body highlighted spatial irregularities in thickness and established correlations with the supra-layer cover, consisting of Ypresian and Lutetian flint limestones and Miocene sands. Chemical element analysis revealed content variations between the two dominant phosphate types, beige and dark gray, with isotener maps illustrating geochemical heterogeneities within the phosphate layer. Bi-variable statistical analyses provided additional insights, demonstrating strong positive correlations between P_2O_5, CaO, and SiO_2, while MgO showed a negative correlation. Principal Component Analysis (PCA) further identified three distinct geochemical associations, corresponding to the phosphate material, the organic and dolomitic matrix, and the clay material. These findings offer valuable insights for optimizing selective phosphate exploitation. By identifying spatial thickness variations, geochemical properties, and facies transitions, the study enables precise targeting of high-grade zones, reduces waste, and supports strategic planning for sustainable resource management at the Djemi-Djema Est deposit.

Received Date: 09.05.2024
Accepted Date: 08.08.2025

Citation Info: Boulemia, S., Hadji, R., Amara, F., Abid, R., Hamed, Y. 2026. Mineralogical and geochemical characterization of Thanetian-Ypresian Phosphatic Layers in the Djemi-Djema Deposit. Bulletin of the Mineral Research and Exploration 179, 1-20. https://doi.org/10.19111/bulletinofmre.1793721

**Corresponding author: Salim BOULEMIA, boulemiasalim51@gmail.com*

1. Introduction

The sustainable utilization of Earth's natural resources remains a critical concern in modern civilization (Kallel et al., 2017; Barra et al., 2019; Wang et al., 2019). Mineral resources, particularly phosphate rocks, play a pivotal role across various industries, serving as indispensable inputs for fertilizer production, animal feed, cosmetics, electronics, and even as potential sources of uranium due to their naturally high uranium content (Cook and Shergold, 1984; Pufahl and Groat, 2017; Tulsidas et al., 2019; Daneshgar et al., 2018). Despite their importance, the exploitation of phosphorites is fraught with challenges, including environmental and radiological concerns stemming from heavy metal content, which necessitates a comprehensive understanding of their geological, mineralogical, and geochemical characteristics (Bezzi et al., 2012; Bouzenzana, 2013; Boumaza et al., 2021).

Phosphorites, primarily composed of apatite-group minerals such as carbonate-fluorapatite (collophanite or francolite), fluorapatite, and hydroxylapatite, exhibit varying forms including grains, organic skeletal fragments, and fine crystalline aggregates (El Bamiki et al., 2021). These deposits are enriched with phosphates (26-36% P_2O_5), fluorine (up to 3%), and uranium (60-200 ppm), but also contain impurities such as silica, clays, and gypsum that must be removed during processing (Kechiched, 2017). The quality of phosphate ores is further influenced by the composition of gangue materials, which vary from siliceous to calcareous elements. These factors underscore the need for advanced geological and geochemical analyses to enhance the sustainable exploitation of phosphate resources.

Globally, sedimentary phosphorites of marine origin constitute the majority of phosphate rock production and are critical for meeting the growing demand in agriculture and industry (Filippelli, 2011; Cordell and White, 2011; Desmidt et al., 2015). The Middle East and North Africa (MENA) region, particularly Maghrebian countries, holds some of the world's largest phosphate reserves, with Algeria's Eastern Saharan Atlas estimated at approximately 2.2 billion metric tons (Dassamiour, 2012; Nouioua et al., 2015; Kechiched, 2017; USGS, 2020; Dassamiour et al., 2021; Mahleb et al., 2022). Within this context, the Djemi-Djema-East site, of Paleocene-Eocene age, represents one of the most significant phosphate deposits in Algeria. Located in the southern sector of the Jebel Onk syncline and forming part of the Metlaoui-Gafsa-Onk transboundary basin at the Algerian-Tunisian border, this site is of both geological and economic importance (Mezghache et al., 2004; Gadri et al., 2015; Lassis et al., 2015; Zerzour et al., 2020; Ferhaoui et al., 2022). Despite its long history of exploitation since the late 19th century, many scientific challenges remain in understanding the mineralogical and geochemical characteristics of this deposit (Oussedik et al., 1980; Tahri et al., 2019).

This study addresses these challenges by focusing on the geological, mineralogical, and petro-geochemical characterization of the Djemi-Djema-East phosphate deposit. Specifically, we aim to: Assess the quality of the deposit by analyzing its mineralogical and geochemical properties. And develop a conceptual model to guide future exploration and exploitation strategies.

Contribute to sustainable resource management by integrating scientific insights with practical mining applications.

By providing a detailed analysis of the deposit's phosphate facies and their enrichment potential, this research seeks to bridge the gap between scientific understanding and industrial application. It builds on existing geological studies while incorporating advanced technological tools for resource prospecting and modeling. The outcomes of this work are expected to benefit both the scientific community and the mining industry, ensuring informed decision-making for the sustainable development of this vital resource.

2. Geographical and Geological Settings

The study area is located near the city of Bir El Ater in Tebessa Province, situated in the extreme northeastern part of Algeria, approximately 20 kilometers from the Algerian-Tunisian border (Figure 1). The Jebel El Onk anticline forms part of the northern branch of the southern flexure, marking the transition zone between the Atlas domain and the Saharan

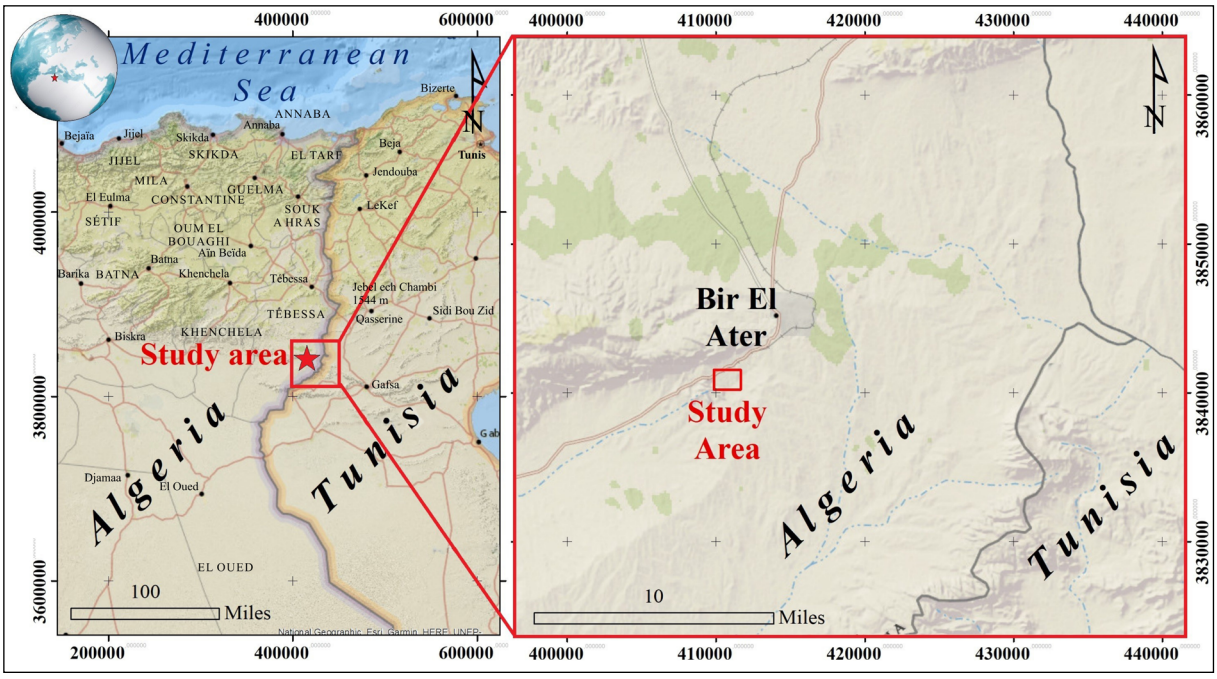

Figure 1- Geographic location of the study area.

platform (Chibani et al., 2022). During the Late Cretaceous to Early Paleogene period, northeastern Algeria was submerged under the southern Tethyan Ocean, as evidenced by widespread shallow marine sedimentary deposits.

The Jebel El Onk mine represents the westernmost extension of the Onk-Gafsa-Metlaoui phosphatic basin, a region known for its significant phosphorite deposits, which are actively exploited by Algerian (SOMIPHOS) and Tunisian (CPG) mining companies. Phosphate deposition in this area primarily occurred between the Late Cretaceous and Eocene, coinciding with the broader phosphogenic events in the Middle Eastern to North African Late Cretaceous-Paleogene phosphogenic province. These deposits exhibit notable similarities in their petrographic characteristics and, to a lesser extent, their geochemical properties, reflecting shared depositional and diagenetic conditions across the region.

The sedimentary succession of the Jebel Onk mining basin is composed of limestones, marls, phosphates, and evaporites, reflecting a range of marine environments from neritic to lagoonal conditions, which were influenced by sea-level fluctuations and local tectonic activity (Hamdadou, 1996). The Maastrichtian represents the base of the Upper Cretaceous to Lower Paleogene sedimentary sequence in this region, characterized by inoceramid limestones. During the early Paleocene (Danian-Selandian), subsidence of the basin accelerated, leading to the deposition of a thick marly horizon. However, subsidence slowed during the early Thanetian, a period marked by black marl shales intercalated with irregular layers of limestone that contain the marine gastropod Clavilithes. The sedimentary sequence then continued with the deposition of thin, clay-rich phosphate layers (Figure 2).

In this phosphatic deposits the late Thanetian to early Ypresian period is marked by the deposition of a substantial phosphate formation, (Cielensky et al., 1988; Prian and Cortiel, 1993). This phospharenite layer is particularly distinctive due to the absence of sterile intercalations, making it a unique and continuous feature within the stratigraphy. The succession is divided into three sub-layers, consistently identified throughout the Jebel El Onk district (Figure 3). The basal sub-layer, approximately 2 meters thick, comprises alternating marl, phosphorites, and dolomite, reflecting an initial phase of deposition. Above it lies the main sub-layer, which is the most prominent, with a thickness ranging from 25 to

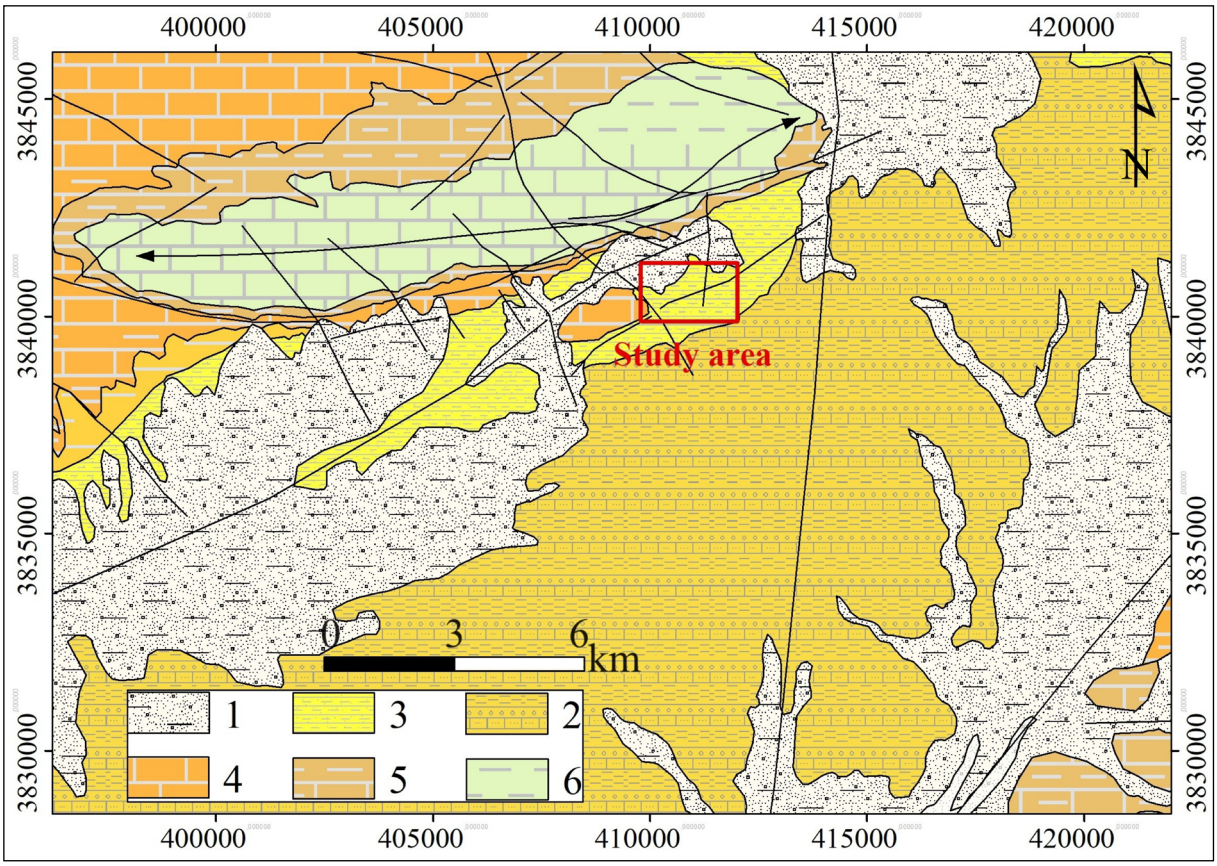

Figure 2- Simplified geological map of Bir El Ater mining basin. [Legend : 1= Quaternary (Holocene): Current and recent alluvium, (sands, gravels, and clays). 2= Mio-Pliocene: Clays and conglomerates, lacustrine limestones. 3= Middle Miocene (Helvetian): Clays, marls, and sandstones. 4= Lower and Middle Eocene (Ypresian and Lower Lutetian): Flinty limestones and marly limestones, sometimes with gypsum. 5= Paleocene-Maastrichtian: Marls and marly limestones. 6= Upper Cretaceous (Campanian and Maastrichtian): Marly unit at the base and various limestones (oolitic, zoogenetic, with flint) at the top].

30 meters. This layer consists predominantly of friable phosphorites embedded in a clay-rich matrix, characterized by dark gray to beige hues. Abundant green glauconite particles are dispersed throughout this matrix, accompanied by numerous fossilized remains of lamellibranchs, gastropods, and fish teeth, including elasmobranch specimens, as documented in systematic studies (Boulemia and Adnet, 2023). Occasional intercalations of marl and dolomite are also observed, contributing to the compositional complexity of this layer. The uppermost sub-layer, ranging from 4 to 6 meters in thickness, is dominated by phosphatic dolomite, indicative of a shallow marine depositional environment. This horizon also includes intercalations of phosphatic limestone and cherty nodules, which are notably associated with fossils of Ostrea multicostata (Strougo, 1976). The marine sedimentary sequence concludes with deposits indicative of a lagoonal environment, represented by white gypsum marls interspersed with phosphate-rich green clays attributed to the “middle Eocene”. These Paleogene marine sediments are unconformably overlain by Miocene deposits, which consist predominantly of terrigenous rocks, marking a significant shift in the depositional environment.

3. Materials and Methods

3.1. Ground Work and Sample Collection

To investigate the geological context and obtain representative phosphatic rock samples from the Djemi-Djema East mining sector, a comprehensive fieldwork campaign was conducted during 2020-2021. A total of 32 rock samples, intended for petrographic and mineralogical analyses, were systematically collected from the main exploitable phosphate layer. This layer is strategically located on the southern

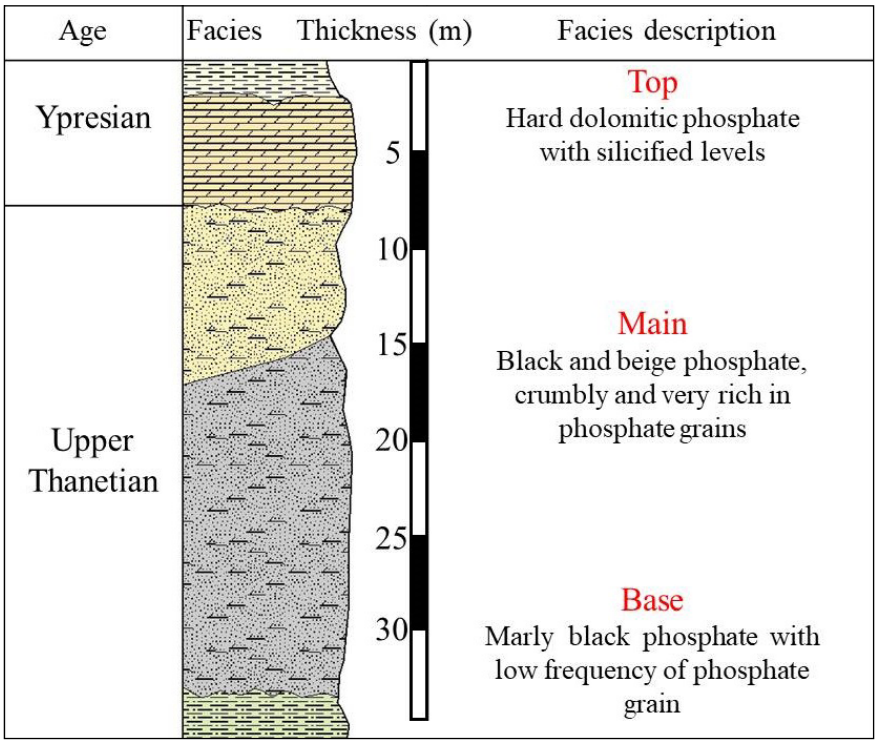

Figure 3- Stratigraphic section with the main phosphorite layer in Djemi-Djema deposit.

flank of the Jebel El Onk anticline, specifically at the exploitation front or western boundary of the Djemi-Djema East sector, which served as the focal point for selective sampling. The sampling strategy was carefully designed to provide a diverse and representative set of phosphatic formations within the study area, enabling detailed petrographical and mineralogical investigations. Additionally, a geochemical approach was employed, utilizing the results from chemical analyses of core samples obtained during the EREM exploration campaign. These core samples were collected systematically from 11 drill holes, designated S-61 to S-17. The sampling procedure involved collecting data at one-meter intervals, covering a cumulative depth of 231.6 linear meters and yielding a total of 232 samples for geochemical analysis. This methodical approach ensured comprehensive coverage and robust data acquisition, forming the basis for in-depth geochemical characterization of the phosphatic deposits.

3.2. Petrographic Analysis

Petrographic studies were conducted using a Leica polarizing optical microscope to examine the structural and textural characteristics of the phosphatic rocks. Thin and polished sections were meticulously prepared from 17 samples representing different phosphate facies (Figure 4). This detailed analysis provided valuable insights into the mineralogical composition, and microstructural features of the phosphatic rocks, enhancing the understanding of their genesis and depositional environment.

3.3. Mineralogical Analysis

X-ray Diffraction (XRD) identification of phosphorites (15 samples of bulk rock) involved a well-defined protocol. X-ray diffraction measurements of the natural samples, in multiphase powder form, were recorded using an X'Pert Pro PANalytical diffractometer operating at 45 kV and 40 mA with Cu K-alpha radiation. Subsequently, the obtained X-ray data were interpreted using the advanced "High Score Plus" software.

3.4. Geochemical Analysis

For the determination of major elements, geochemical analysis was conducted on the collected samples. This process was carried out using Perkin Elmer flame atomic absorption spectrometry, and the

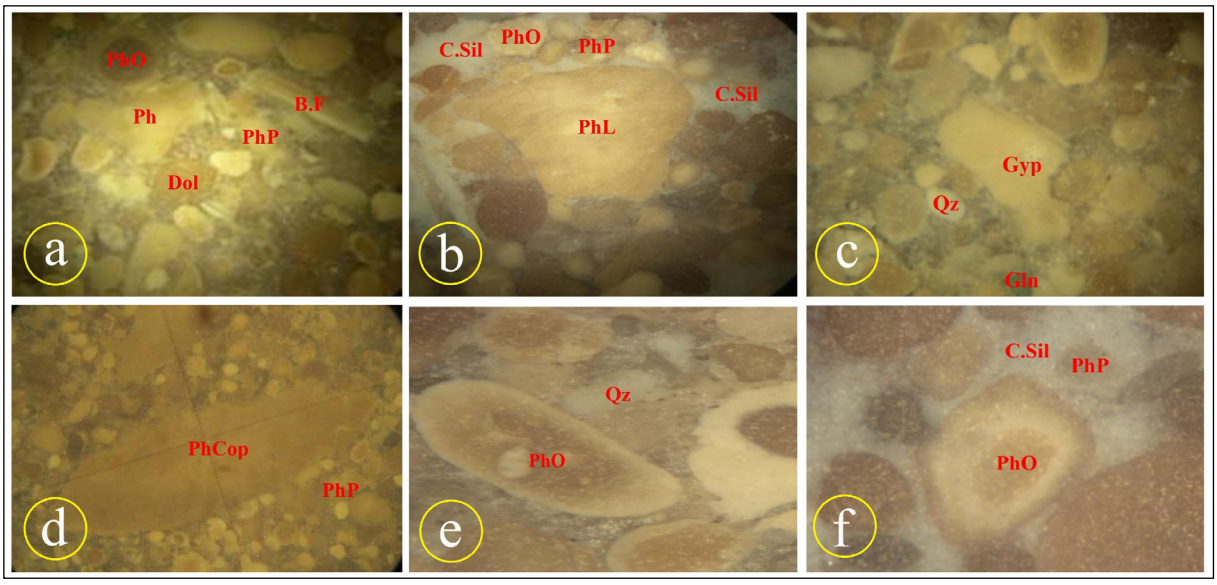

Figure 4- Photographs show the various phosphate components in the phosphorites (polished sections) from the Djemidjma deposit [(PhP) Phosphatic pellet , it show a structureless interior pattern, (PhO), phosphatic ooid ; they may contain multiple cores, and the cores are also coated ooids. (Ph)The amorphous grain aggregated together with phosphatic matrix (possibly collophane). (BF) phosphatized bio-fragment (bone). (C.Sil) siliceous cement. (Cal) calcite cement. (PhL) phosphatic Lithoclast (Gyp) gypsuim (Gln) glauconite (Qz), quartz grains]. a) Phophorite Packstone contains different forms of phosphatic grains and calcareous cement with dolomie rhomboèdre. The grains are mainly phosphatic ooids, pellets, and bio-fragments. b) Irregularly shaped phosphate lithoclast surrounded by light and dark colored pellets in a siliceous matrix. c) Phophorite à texture Packstone, show phosphatic grains with different grain sizes and morphology; an also, du gypsuim , glauconite and Quartz. d) Oval-shaped phosphate coprolite in a grainstone-textured phospharenite. e) Phosphatic ooids contain multiple cores (pellet developed around a multi-component core). f) Phosphatic pellet (multilayer ooids) , coated grains with distinct concentric zonation, consisting of alternating light gray and dark gray phosphatic layers (The darker halos are richer in organic matter).

analysis was performed at the laboratory facilities of SOMIPHOS Company in Bir El Ater city. This phase of the study provided crucial insights into the elemental composition of the phosphatic rocks, contributing to a holistic understanding of their geochemical characteristics.

The geochemical data, encompassing the concentrations of P_2O_5, MgO, CaO, CO_2, and SiO_2 oxides, were utilized for automated mapping. To ensure consistency, arithmetic averages were calculated for each drill core (Table 1). For exemple, in the core S64 and S-70, 28 and 23 samples were collected

Table 1- Average Chemical Composition of the Phosphate Layer in Each Borehole at Djemi-Djema East.

Drill N°	P_2O_5	MgO%	CaO%	CO_2%	FeO3%	SiO_2%	Ri%[22]
S-61	Eroded layer						
S-62	24.34	4.12	45.50	12.40	0.59	1.11	1.53
S-63	24.30	4.20	44.00	11.70	0.61	0.83	2.04
S-64	24.84	3.41	44.39	9.01	0.51	2.23	3.02
S-65	25.11	3.53	45.91	11.22	0.47	2.13	2.81
S-66	25.47	3.25	45.47	9.39	0.56	1.21	2.11
S-67	26.21	2.55	46.54	9.31	0.48	0.79	2.54
S-68	25.86	2.74	45.74	8.63	0.55	2.22	3.13
S-69	26.09	3.23	45.21	10.06	0.54	1.64	3.19
S-70	25.28	2.32	44.19	8.86	0.56	1.86	2.47
S-71	25.87	3.25	45.12	9.68	0.54	1.60	3.03
Average	25.34	3.27	45.22	10.07	0.54	1.56	2.59

respecrevely from the main exploitable phosphate layer within depths ranging from 78 m to 107 m (Table 2). The mean values were then computed based on the chemical contents of all samples from each drill core. The interpolation and mapping processes were performed using Surfer (V10) and ArcGIS software, employing kriging as the geostatistical model. This method allowed for the precise spatial interpolation and visualization of geochemical data. Multivariate statistical analysis was applied to examine the interrelationships among the measured chemical elements. Principal Component Analysis (PCA), a method of factor analysis, was employed to construct new theoretical variables (factors) that capture the maximum possible information from the data matrix in a condensed form. This approach provided deeper insights into the geochemical variations and underlying patterns within the dataset.

4. Results and Discussion

4.1. Morphology of the Phosphate Layer

The Djemi-Djema East deposit, forming the eastern pericline of the deposit, was initially identified

Table 2- Results of chemical analyses for Boreholes S-64 and S-70.

Depth	P_2O_5	MgO	CO_2	CaO	SiO_2	Depth	P_2O_5	MgO	CO_2	CaO	SiO_2
S-64						**S-70**					
78.35	22.70	4.18	11.11	42.50	5.51	86.58	22.09	3.36	11.92	46.00	3.65
79.35	25.66	2.85	8.13	44.88	2.41	87.58	29.17	1.89	5.69	47.88	0.76
80.35	25.20	2.85	8.67	44.88	2.46	88.58	29.31	1.05	4.60	48.63	0.52
81.35	25.20	2.94	8.40	44.88	2.27	89.58	26.17	0.84	4.87	48.34	0.60
82.35	25.36	3.04	8.67	44.75	1.94	90.80	27.86	0.63	5.96	48.34	1.16
83.35	24.80	2.85	9.84	44.88	1.95	92.03	25.84	2.94	8.40	46.29	1.33
84.35	23.10	4.84	11.38	43.56	1.27	93.28	26.59	1.89	8.13	47.17	1.43
85.35	24.80	4.08	10.03	44.62	0.78	94.54	19.46	5.46	23.03	46.29	2.32
86.60	26.40	3.23	8.40	45.94	0.59	95.80	27.71	3.15	6.23	45.70	1.57
87.85	24.10	4.84	10.37	43.96	1.07	96.94	25.36	2.94	8.13	44.53	2.45
89.10	23.50	4.37	10.54	44.09	1.20	98.04	26.20	2.10	7.85	46.29	2.15
90.35	22.30	5.13	12.74	43.56	1.10	99.04	24.64	3.57	9.48	44.24	2.45
91.35	28.40	1.52	5.96	46.73	0.84	100.04	24.88	1.68	8.67	45.70	1.82
92.35	10.30	11.21	25.20	36.43	0.42	101.04	26.39	1.26	7.58	45.70	1.85
93.35	28.50	3.42	8.54	44.75	1.22	102.04	24.54	1.89	8.94	44.82	2.83
94.35	26.10	2.56	7.05	44.88	1.50	103.04	23.34	2.73	9.75	44.82	1.80
95.35	23.60	4.75	10.57	43.56	1.62	104.52	26.51	1.89	7.31	46.29	2.17
96.35	24.20	4.18	9.35	43.56	1.85	105.61	25.11	2.10	9.75	45.70	1.49
97.35	26.30	2.56	7.18	44.75	1.87	106.70	27.44	1.26	7.04	46.88	1.51
98.35	25.90	3.04	7.86	44.35	1.87	107.97	26.85	2.10	8.67	46.88	1.06
99.35	27.40	2.09	6.23	46.60	2.05	108.88	25.38	2.52	9.21	46.00	1.24
100.35	27.60	2.18	6.50	46.07	0.81	109.97	24.56	2.52	10.02	45.41	1.89
101.35	27.10	1.80	6.23	46.20	1.21	111.00	21.07	3.57	12.73	44.24	3.92
102.35	27.44	1.52	5.42	46.99	1.65						
103.35	26.70	2.47	7.32	45.67	1.47						
104.35	27.80	3.80	10.03	44.09	2.38						
105.35	24.00	1.61	5.69	46.07	2.56						
106.35	24.10	1.80	5.28	40.00	7.73						

by L'E.R.E.M. in 1986 through the deployment of 11 core drills (S61 to S71) at a mesh size of 500x600 m (Figure 5).

The iso-thickness map of the stratiform phosphate body reveals a consistent total thickness ranging between 16m and 31m, extending seamlessly between marls and flint limestones. This singular layer, devoid of sterile interlayers, exhibits remarkable uniformity over the entire area, except for notable irregularities observed at the locations of core drills S65 and S67, with a complete absence towards S61 (Table 3, Figure 5).

The supra-layer coverage of phosphate, primarily composed of easily strippable Miocene sands, demonstrates significant variability, ranging from 7m to 136m. Despite this variability, it intriguingly mirrors

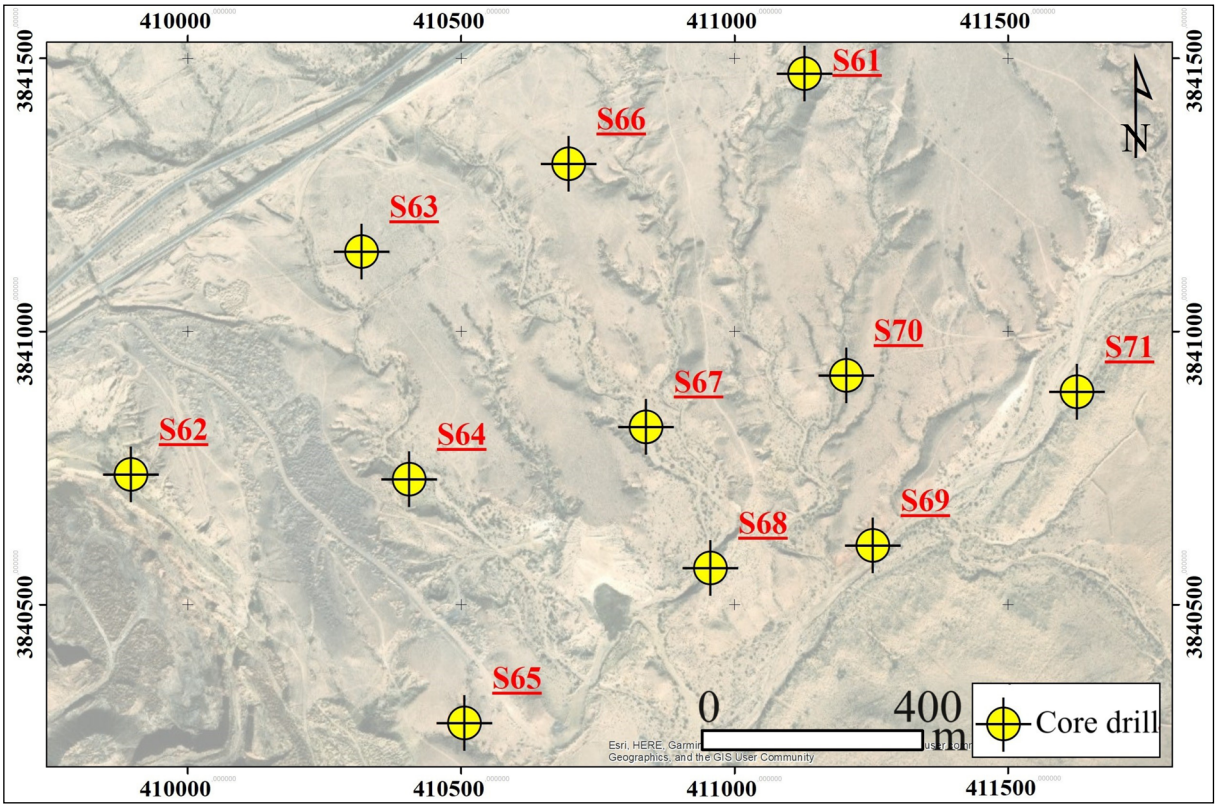

Figure 5- Geographic location of the 11 Core drill in the study area (WGS 84, UTM 32 N).

Table 3- Analytical data by Drill Hole used for the preparation of Isopach and Isobath Maps.

Drill Hole	Coordinates			Thickness of the Productive Layer	Thickness of the Overburden	Thickness of the Sterile Overburden	Elevation of the Top of the Phosphate Layer
Number	(X)	(Y)	(Z)				
S-61	987.93	170.43	813.00			126.7	
S-62	986.75	169.61	822.86	31.30	80.40	66.7	766.2
S-63	987.15	170.05	815.72	25.80	106.40	66.1	711.5
S-64	987.26	169.64	809.10	29.00	77.30	28.0	789.4
S-65	987.39	169.2	782.08	8.30	111.30	15.5	677.8
S-66	987.52	170.23	813.45	28.00	82.10	74.5	734.9
S-67	987.69	169.76	799.53	16.50	81.00	37.0	731.8
S-68	987.82	169.51	786.00	26.60	91.20	32.0	703.5
S-69	988.11	169.57	779.27	30.00	129.10	72.2	654.2

the contours of the underlying layer, accentuating the geological nuances of the phosphate deposit (Figure 6). This observation suggests a complex interplay of geological factors influencing the distribution and thickness of the Miocene sands, possibly related to the underlying structural features.

These findings underscore the significance of understanding the primary phosphate layer, and the overlying supra-layer cover, providing valuable insights into the geological dynamics and potential variations in exploitable resources within the Djemi-Djema East deposit. Further investigations are warranted to unravel the intricate geological processes shaping the observed irregularities and variations in thickness, contributing to a more comprehensive comprehension of this phosphate-rich region.

4.2. Mineralogical Analysis

The XRD analysis of 16 representative phosphate samples (bulk rock) from the unique phosphatic layer in the Djemi-Djema East sector reveals a diverse mineralogical composition, reflecting the geological complexity of the region. The samples, collected systematically from the exploitation front's base to its uppermost section in the western part of the study area, exhibit a rich array of mineral phases, including phosphates, sulfates, sulfides, tectosilicates, phyllosilicates, and native elements such as graphite (Figure 7). These findings underscore the intricate mineral assemblages embedded within the phosphorites of Djemi-Djema. XRD analysis highlights apatite as the predominant mineral group, with hydroxylapatite frequently present, either alone or in association with francolite, fluorapatite, and dahllite. Carbonates such as calcite and dolomite, silica in the form of quartz, and clay minerals like palygorskite are also identified. Gypsum, a secondary mineral likely formed through meteoric water circulation, is closely associated with the phosphorites. The presence of graphite in certain phosphatic rocks suggests highly reducing conditions during their formation. This mineralogical composition aligns with XRD diffractograms of Paleocene-Eocene phosphates from the northern basin deposits of El Kouif and Djebel Dhyr (Boulemia et al., 2015). The consistency of these findings highlights the regional

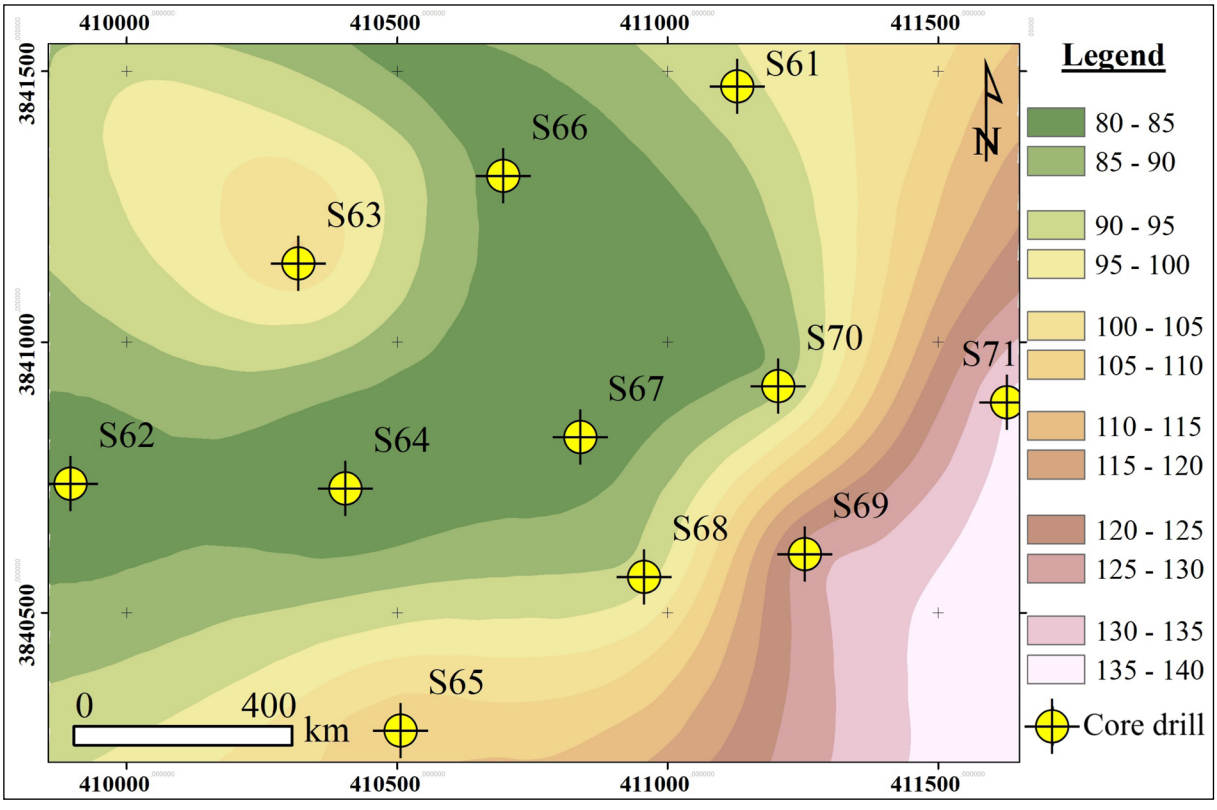

Figure 6- Iso-paque map of the total thicknesses of the sterile cover.

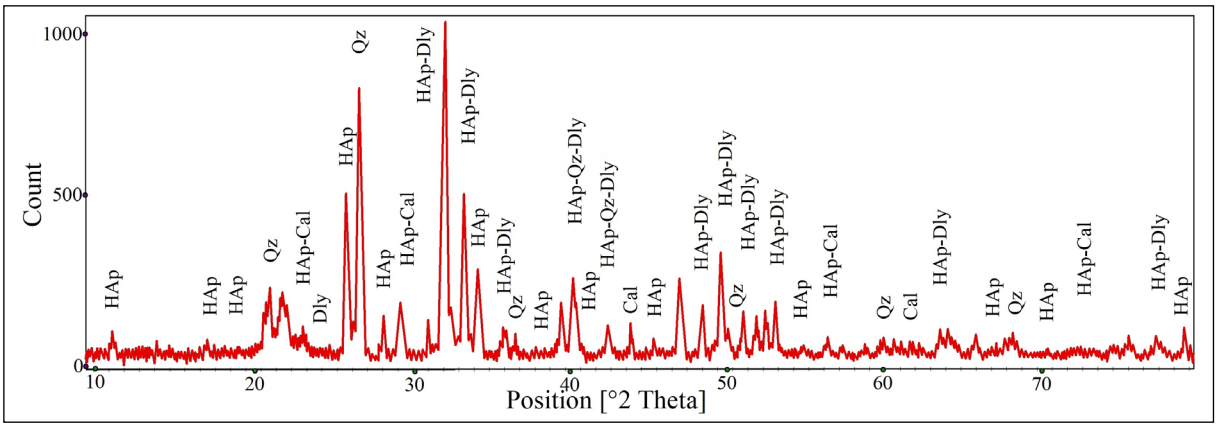

Figure 7- X-Ray Diagram with Apatitic components, carbonates, and siliceous gangue in samples (HAp: Hydroxyapatite, Cal: Calcite, Dly: Dahlite, Qz: Quartz).

significance of the mineral phases. Furthermore, the observed mineral assemblages reflect a broader pattern common to Paleocene-Eocene phosphorites across the MENA region. While the mineralogy of phosphorites is relatively straightforward, the variability arises primarily from differences in apatite types and the proportions of allochems in clay or carbonate cements (Abed et al., 2005; Ounis et al., 2008; Ben Hassen et al., 2011; Kocsis et al., 2014*a, b*; El Ayachi et al., 2016; Garnit et al., 2017; Jaballi et al., 2019; El Bamiki et al., 2020; Zhang et al., 2021; Abou El Anwar and Abd El Rahim, 2022). These analyses provide a valuable comparative reference for geological studies in neighboring regions, contributing to an understanding of phosphorite mineralogy in the broader geological context.

4.3. Petrographic Observations

The petrographic analysis included a variety of samples, such as sandy phosphates, calcareous phosphates, and phosphatic mudstone rocks. These samples exhibit a grainstone facies texture; characterized by a high proportion of allochems relative to the matrix, underscoring the allochem-rich composition of the main phosphatic layer (Figure 8a).

Using a polarizing microscope, detailed observations identified various phosphate allochems (Figure 8b). Coprolites, typically larger than 250 µm and occasionally several millimeters, displayed diverse colors ranging from light yellowish to dark tones, indicative of varying organic matter content (Boulemia et al., 2015). Pellets, often termed pseudo-ooliths, were notable for their sub-rounded to well-rounded shapes, smooth surfaces, and lack of concentric structures. Their colors varied from brownish white to dark brown or black, depending on the organic content (Boulemia et al., 2021). Intraclasts, angular to irregular fragments with internal microstructures reaching up to 1 cm in size, were reworked and embedded in the matrix. Biogenic phosphates, such as fossil fish teeth belonging to Elasmobranch families, were well-preserved and entirely composed of phosphate, (Boulemia et al., 2023).

Non-phosphate components were also observed, including green glauconite grains, quartz occupying intergranular voids, and bone debris characterized by elongated calcite structures, some of which were replaced by microcrystalline quartz. Partially destroyed oyster shells (Ostréa Multi Costata) composed of calcite and dolomite, and calcite grainstones, appeared as rhombohedral crystals and bands. The cement was primarily calcareous (sparite) and occasionally siliceous, a result of diagenetic calcitization and partial silicification (Dar et al., 2017).

The studied samples ranged in color from light beige to very dark brown, with medium to coarse fractions embedded in matrices of clay minerals (friable rock) or carbonates (hard and compact rock). Occasionally, siliceous or collophanic textures were present. All samples from the main phosphatic layer exhibited a clear dominance of allochems, including coprolites, pellets, and intraclasts, over the matrix (Figure 8b).

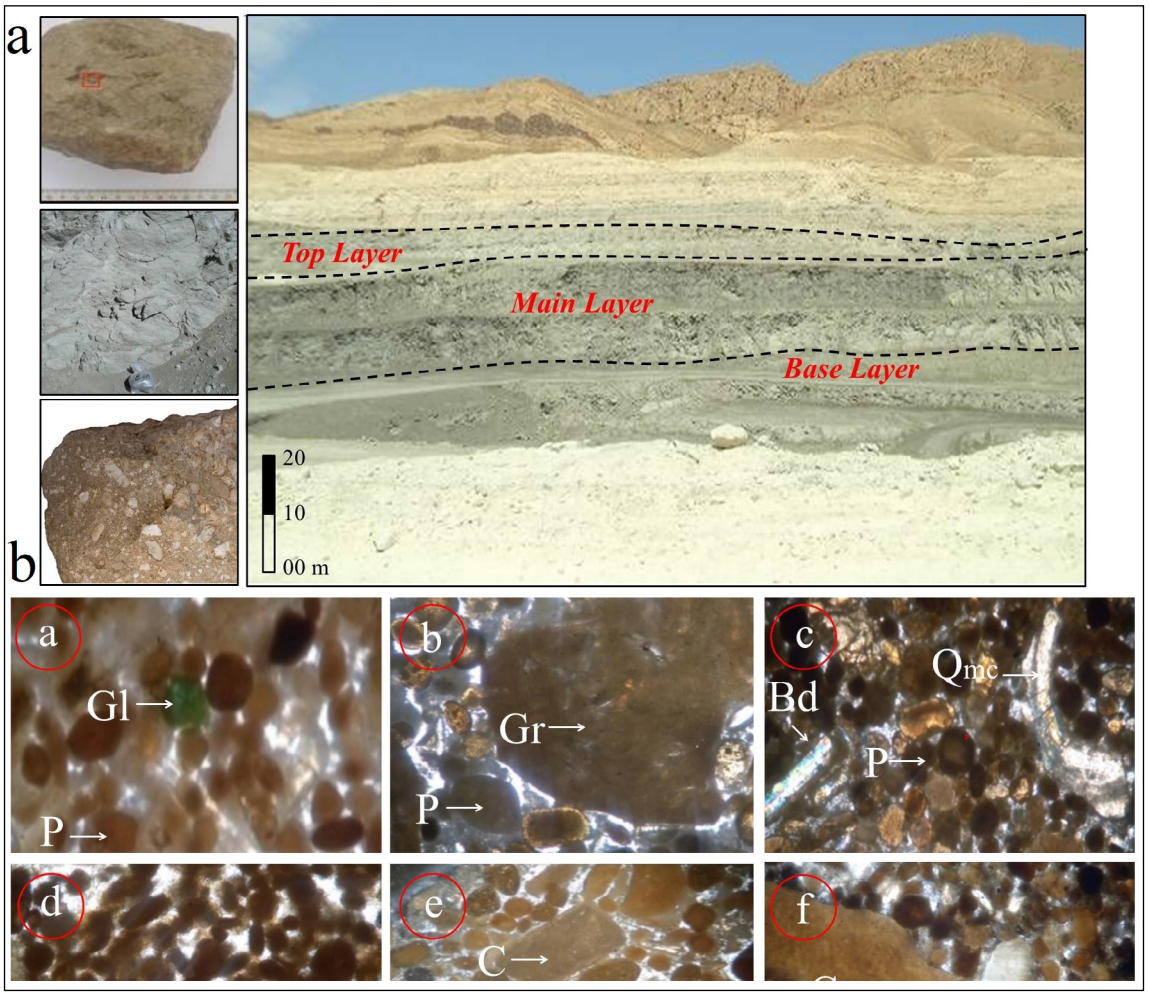

Figure 8- a) Outcrops and Rock Samples Used for the Petrographic Study, b) Phosphate Facies and Allochems, a- Pel-phosphorites Featuring Glauconite Grains (100µm). b- Intraclasts (Granule) and Organic-Rich Pellets (Brown to Dark) (200µm). c- Oyster or Arc Bivalve and Calcitic Bone Fragments in Grainstone Texture Phosphorite (100µm). d- Gray-Black Ore with Phosphorite Grains Rich in Organic Matter (100µm). e- Light Ore, Beige-Brown, Displaying Heterometric Apatite Grains (100µm). f- Hard Ore with Coarse, Brown to Beige Apatite Grains Accompanied by Quartz Grains (150µm).

These characteristics align with the petrogenesis of phosphates found in nearby regions, such as Djebel Dhyr and the El Kouif deposit (Boulemia et al., 2021).

Three distinct sub-facies were identified, offering potential for selective phosphate exploitation in the sector. The first sub-facies, gray-black soft ore with fine grains, primarily consisted of homometric phosphalutite grains, 80% of which were finely punctuated with organic matter. This texture, indicative of anoxic conditions during phosphorite genesis, resembled grainstone with thin clay borders and sparse dolomitic rhombohedra (Boulemia et al., 2023). The second sub-facies, light beige to brown ore with a relatively hard texture, featured heteromeric grains (fine to medium) dominated by phosphate pellets. These sub-jointed to jointed textures with calcite inclusions represented high-grade phosphorites, likely linked to climate and sea-level changes during phosphorite deposition episodes (Boulemia et al., 2021). The third sub-facies, hard ore with coarse grains in a brown-beige hue, exhibited heterogeneous, non-joined grains with an abundance of coprolites, broken bones, and compound pellets. Glauconite, detrital quartz, and large gypsum crystals were commonly found, set within well-developed dolomitic cement.

This petrographic characterization of the phosphatic rocks in the Djemi-Djema East sector highlights their texture, composition, and genesis.

4.4. Geochemistry of the Phosphate Layer

4.4.1. Chemical Composition and Spatial Distribution

The chemical composition study unveiled noteworthy observations derived from the average content analysis of essential elements (P_2O_5, MgO, CaO, SiO_2, and CO_2) in each core drilling.

P_2O_5 Content and Iso-Content Map:

P_2O_5 contents consistently range from 24.33% (S63) to 26.2% (S67), averaging around 25.18% across Djemi-Djema East. The P_2O_5 iso-content map delineates an oval structure with a major N-S axis, highlighting a peak value of 26.21% at the S-67 core drill. Gradual decreases are observed towards the west (S62 core drill) and the extreme east (S70 survey) with values of 24.34% and 25.28%, respectively. Higher P_2O_5 concentrations signify an increased abundance of apatite constituents (Figure 9a).

MgO Content and Iso-Content Map:

Average MgO contents fluctuate between 2.32% (S70) and 4.20% (S63), averaging at 3.25%, indicating

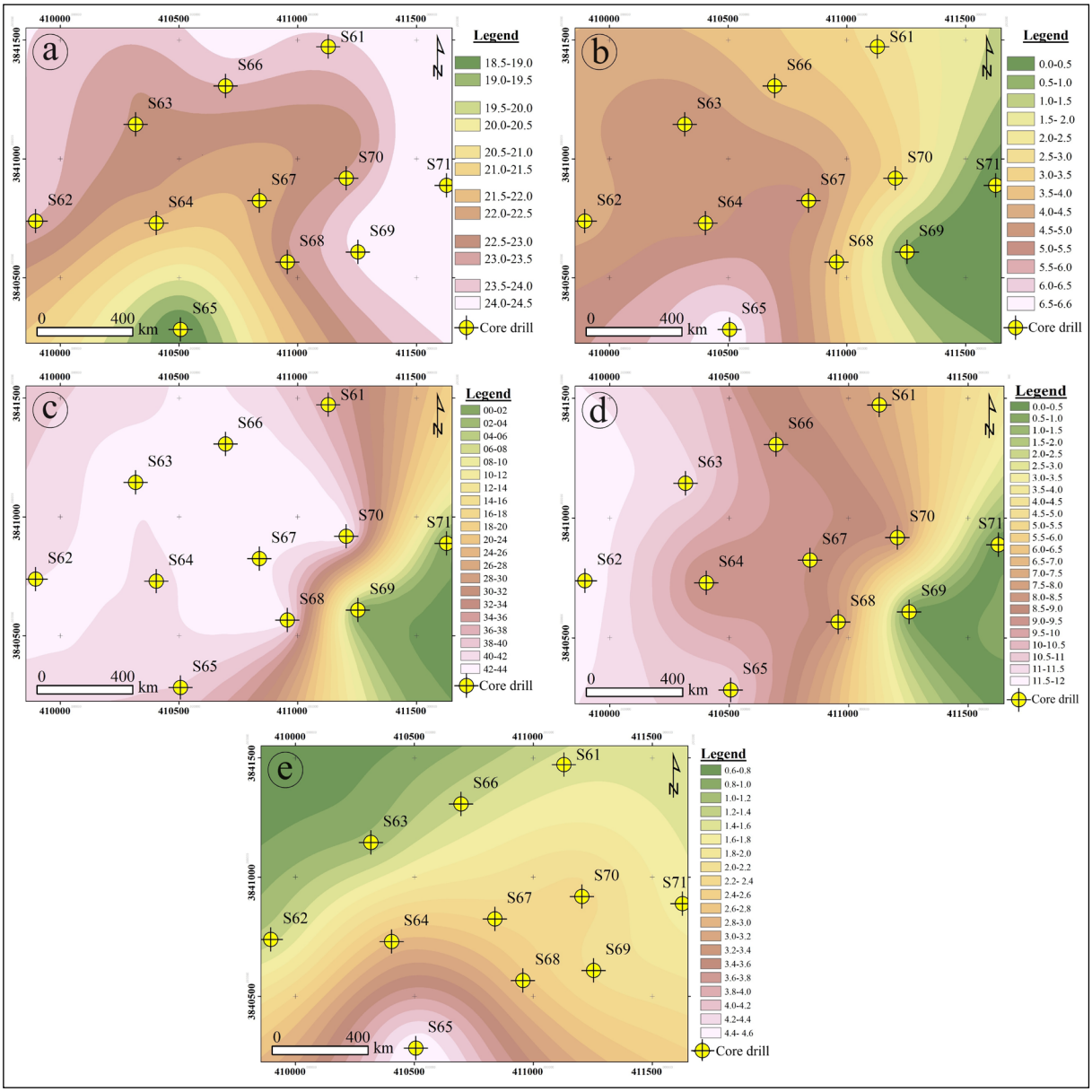

Figure 9- a) Phosphorus (P_2O_5) iso-content map, b) Magnesium (MgO) iso-content map, c) Calcium (CaO) iso-content map, d) Carbon dioxide (CO_2) iso-content map, e) Silice (SiO_2) iso-content map.

an incipient dolomitic cement. The MgO iso-teners map portrays a longitudinal decrease from the east to the west (Figure 9 b).

CaO Content and Iso-Content Map:

CaO values show a narrow range, varying from 44.19% (S70) to 46.54% (S67). The western part of the deposit, centered around S63, exhibits a minimum content of 44%. The isoteners map indicates a concentric structure with increasing contents in all directions from the epicenter (S63), (Figure 9c).

CO_2 Content and Iso-Content Map:

Average CO_2 contents range between 8.63% (S68) and 12.4% (S62), signifying a notable presence of organic matter. The CO_2 iso-teners map displays a west-to-east decrease, except for a slight increase from S64 to S67, (Figure 9d).

SiO_2 Content and Iso-Content Map:

Average SiO_2 contents, relatively low, vary from 0.83% (S63) to 2.22% (S64). The SiO_2 iso-contents map illustrates a south-to-north decrease, with a pronounced variation between S63 and S64 core drills, (Figure 9e).

4.4.2. Geochemical Composition and Vertical Variation

To unravel the nuanced vertical chemical intricacies within the phosphate layer, we conducted a thorough analysis along two core drills, exemplified by profiles (S70) and (S64) (Figure 10, Table 4). These profiles reveal subtle chemical fluctuations at the layer's extremities and midpoint, predominantly aligning with their respective survey averages. The key observations unfold in the dynamics of P_2O_5, CaO, MgO, CO_2, and SiO_2:

-P_2O_5, CaO, MgO, CO_2, and SiO_2 Dynamics:

Profiles of P_2O_5 and CaO exhibit closely mirrored trends, indicating a shared chemical behavior. MgO contents align with CO_2, while SiO_2 displays a comparatively lesser correlation. These variations authentically mirror localized shifts within diverse phosphate facies.

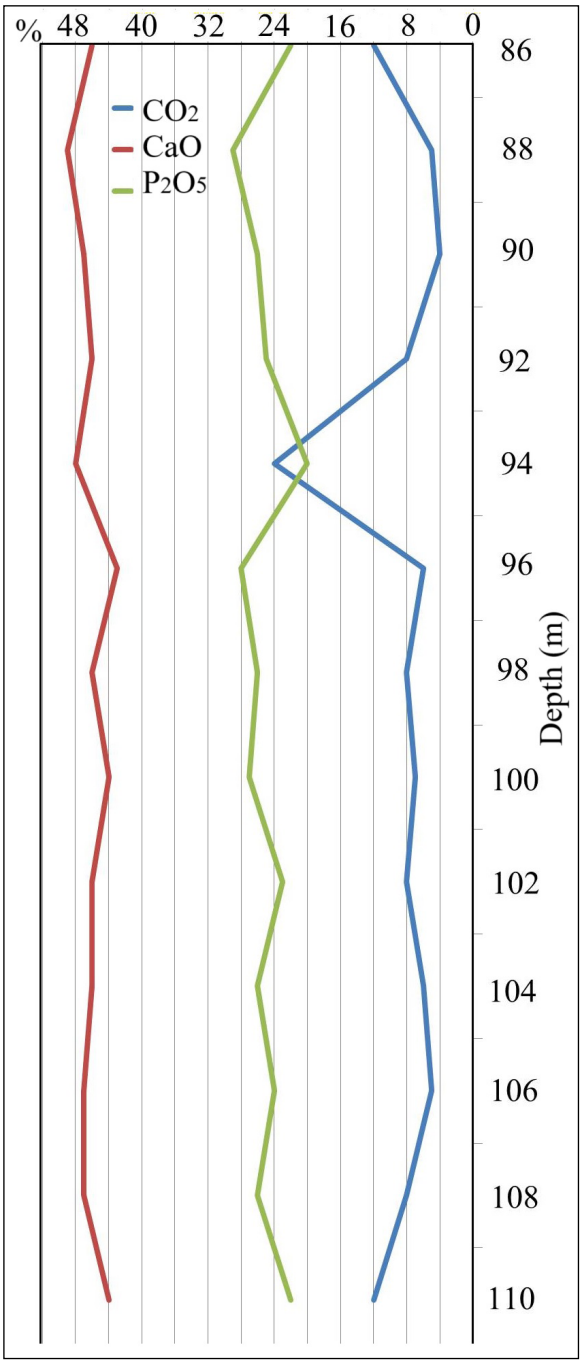

Figure 10- P_2O_5, CaO and CO_2 Oxides along drill SC-70 in the Phosphatic Layer of Djemi-Djema East.

-Vertical dynamics along core drills:

Core Drill (S70): Vertical analysis along this drill reveals consistent chemical behavior at the layer's top, base, and middle, with fluctuations aligning closely with average values.

Core Drill (S64): Similar to (S70), profiles at (S64) display three discernible peaks representing the layer's

Table 4- SiO_2 and MgO Oxides along drill SC-70 in the Phosphatic Layer of Djemi-Djema East.

Depth(m)	86	88	90	92	94	96	98	100	102	104	106	108	110
SiO_2 (%)	3.7	0.6	0.8	1.3	2.4	1.9	2.2	2.0	2.8	2.1	1.9	1.2	2.2
MgO (%)	3.5	1.0	0.7	3.1	2.2	5.5	3.2	2.3	2.0	1.9	2.1	1.3	3.8

top, base, and middle. However, chemical deviations remain modest, encapsulated within survey averages.

-Interpretations:

The synchrony between P_2O_5 and CaO profiles implies an intertwined chemical behavior, shedding light on the interdependence of these elements within the phosphate layer. P and Ca are the two major elements making the framework of the CFA mineral. However, the presence of a substantial amount of calcium also is in the carbonates as calcite and dolomite. Apparently, Ca-sulfates play a minor role (Boulemia et al., 2023).

The resemblance between MgO and CO_2 profiles suggests a notable degree of chemical association, contributing to our understanding of the layer's geochemical intricacies. The lower MgO content indicates that little dolomitization has occurred, and can be attributed to the formation of the phosphatic grains in low MgO seawater (Baioumy, 2007). However, Carbon characterizes both carbonates and organic matter.

The distinct behavior of SiO_2 underscores its unique role in the chemical composition dynamics, standing apart from the closely correlated elements. SiO_2 may indicate the presence of phyllosilicates in phosphatic rocks of Djemi-Djema east.

-Significance:

These findings underscore the efficacy of vertical chemical profiling in unraveling nuanced variations within the phosphate layer, providing crucial insights for refining our understanding of localized changes in different phosphate facies. In essence, the observed chemical dynamics along core drills contribute significantly to our comprehension of intricate geochemical variations within the phosphate layer, offering valuable insights into localized shifts within distinct phosphate facies.

4.5. Correlation Between Chemical Elements

We correlate between chemical elements in Djemi-Djema East phosphorite. Table 5 illustrates the matrix correlations among major elements, providing valuable insights into their relationships. The P_2O_5 contents exhibit a strong negative correlation with MgO (-0.86) and CO_2 contents (-0.745), while displaying a positive correlation with SiO_2 (0.52) and CaO (0.63). SiO_2, in turn, demonstrates a notable negative correlation with MgO (-0.628), with weaker correlations observed with CaO and thicknesses. The correlation matrix serves as a comprehensive reference, revealing intricate associations between key chemical components within the phosphatic layer. These correlations contribute to a nuanced understanding of the chemical dynamics and interactions shaping the composition of Djemi-Djema East phosphorites.

The analysis reveals a clear negative correlation between P_2O_5 (a key component of apatite) and MgO, CO_2, and SiO_2, which are indicative of siliceous phases and clay minerals. This relationship suggests

Table 5- Correlation Matrix between major elements in phosphorites of Djemi-Djema East.

	P_2O_5	SiO_2	CaO	MgO	CO_2	Thicknesses (m)
P_2O_5	1	-0.526	**0.632**	**-0.863**	**-0.745**	-0.385
SiO_2		1	0.240	**-0.629**	**-0.628**	-0.326
CaO			1	-0.263	-0.360	-0.493
MgO				1	**0.868**	0.163
CO_2					1	-0.075
Thicknesses (m)						1

that as phosphate rock becomes more mineralized, the clayey, siliceous, or dolomitic matrix is less developed. The CaO/P_2O_5 correlation highlights a significant and positive relationship, indicating that higher P_2O_5 content corresponds to increased apatite presence. However, as calcium is a constituent of both apatite and carbonates (such as calcite and dolomite), analyzing the CaO/P_2O_5 behavior provides insights into the role of carbonates in the phosphate rocks.

The MgO content, representing the dolomitic exogenous gangue, shows a strong negative correlation with P_2O_5 (r = -0.863), indicating a marked antagonism between apatite and magnesium-bearing minerals. This inverse relationship may reflect diagenetic processes, where MgO is progressively replaced by P_2O_5 in phosphorites (Boulemia et al., 2021). Additionally, calcite tends to be replaced by dolomite during these diagenetic transitions.

Correlation diagrams further emphasize the antagonistic relationships between CaO/MgO and CaO/SiO_2. These patterns suggest that carbonates, or biogenic contributions such as tests of organisms, as well as anhydrite or gypsum, dilute clay minerals within the matrix (Baioumy, 2007). These findings offer valuable insights into the geochemical and mineralogical evolution of phosphate deposits.

4.6. Interpretation of Principal Component Analysis (PCA) Results

The outcomes of the Principal Component Analysis (PCA) were examined and outlined. Key revelations from Table 5 underscore the pivotal role of the first three factors (F1, F2, and F3), collectively capturing a substantial 91.90% of the information. In contrast, factors F4 and F5 contribute a relatively smaller portion, representing only 8% of the information.

The interpretation of the correlation circles in Figure 11 unravels three distinct associations among the elements:

Phosphate Material (P_2O_5 and CaO association):

Exhibits a negative correlation with loading factors F1.

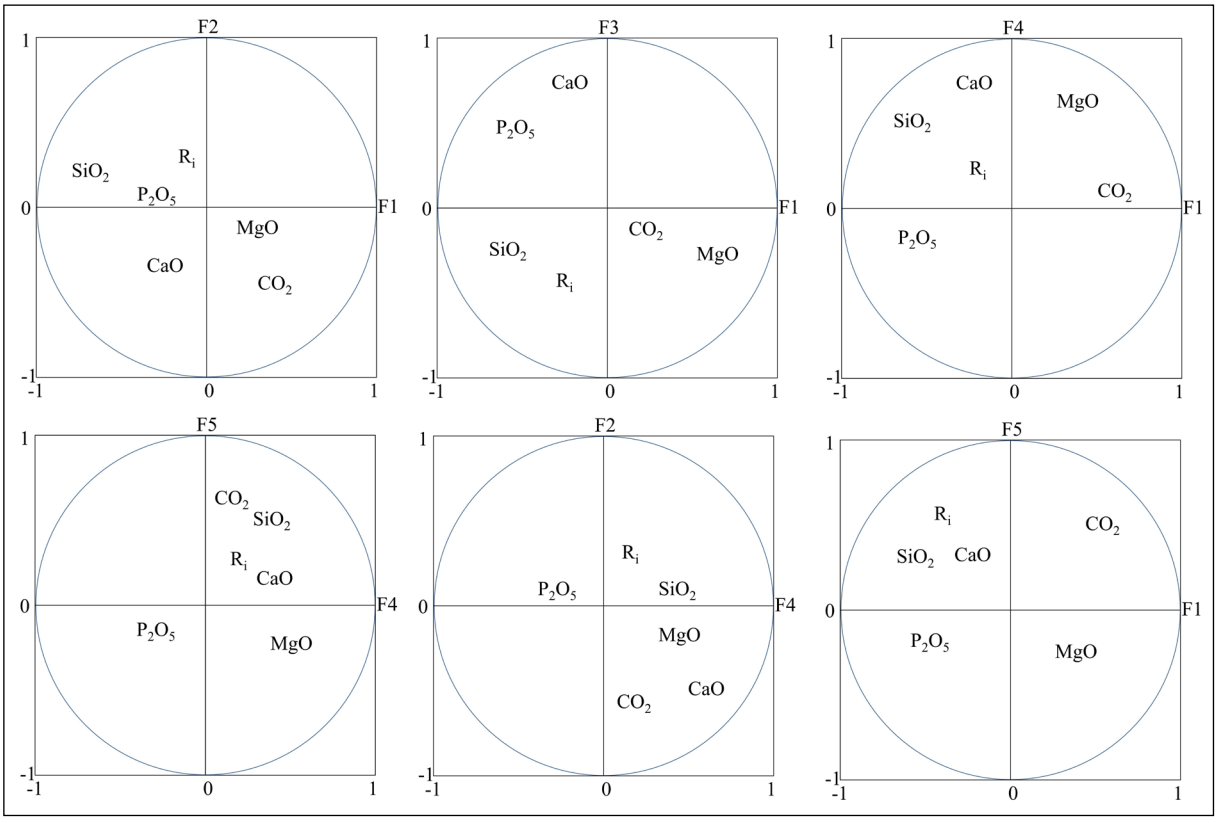

Figure 11- Correlation circles on the Djemi-Djema Est data.

Demonstrates a positive correlation with loading factors F3.

This association is identified as representative of the phosphate material within the samples. Its Apatite group which is expressed in pellets, coprolites, and fossil fish teeth.

Organic and Dolomitic Matter (CO_2 and MgO association):

Shows a positive correlation with loading factors F1.

Displays a negative correlation with loading factors F3.

This association signifies the presence of organic and dolomitic matter in the Carbonated analyzed samples; it's the ortochem or cement embeding the phosphate material.

Clayey Material (SiO_2 and Ri association):

Reveals a negative correlation with loading factors F1.

Displays a negative correlation with loading factors F3.

This association indicates the presence of clayey material or siliceous cement bandes in the samples or even quartz nuclei within the pellets. The insights encapsulated in the correlation circles provide a nuanced understanding of elemental associations within Djemi-Djema Est phosphates. These delineations hold substantial promise for guiding the selective exploitation of phosphates in this region. Additionally, the loading factors and cumulative variances presented in Table 6 offer a comprehensive overview of each element's contribution to the principal components, facilitating the interpretation of the PCA results.

The PCA analysis elucidates the complex interrelationships among elemental variables in the Djemi-Djema Est dataset, providing valuable insights into the underlying chemical associations that may inform geological interpretations. A key finding is that phosphorus pentoxide (P_2O_5) exhibits a strong positive loading on the third factor (F3) at 0.468, while simultaneously registering a negative loading on the first factor (F1) at -0.404. This pattern indicates that P_2O_5 is predominantly linked to F3, suggesting its significant role within that specific context. In contrast, silicon dioxide (SiO_2) displays substantial negative loadings on both F1 (-0.402) and F3 (-0.392), implying an inverse relationship; as SiO_2 levels rise, the influence of these factors may weaken.

Calcium oxide (CaO) presents a dual behavior, with a strong negative loading on F2 (-0.468) and a positive loading on F3 (0.513). This suggests that CaO is intricately tied to transitions between these factors, illustrating its multifaceted role within the dataset. Magnesium oxide (MgO) and carbon dioxide (CO_2) also show mixed loadings across the factors, with MgO contributing positively to F1 (0.382) and CO_2 making a notable positive contribution to F5 (0.437). These mixed loadings highlight the distinct chemical roles that these oxides play in various geological

Table 6- Principal Component Analysis (PCA) Loadings for Elemental Variables (Oxides).

Loading Factors	F1	F2	F3	F4	F5
Own values	L1=4.611	L2=1.703	L3=1.037	L4=0.354	L5=0.150
Cumul. Variances	57.60%	78.90%	91.90%	96.30%	98.20%
P_2O_5	-0.404	0.035	0.468	-0.130	-0.030
SiO_2	-0.402	0.069	-0.392	0.359	0.299
CaO	-0.234	-0.468	0.513	0.519	0.203
MgO	0.382	-0.301	0.282	0.342	0.290
CO_2	0.352	-0.473	-0.103	0.055	0.437
Ri	0.388	0.142	0.441	0.144	0.283

contexts. Additionally, the variable Ri shows positive contributions across several factors, particularly F1 (0.388) and F3 (0.441), emphasizing its broad relevance in the chemical framework.

A closer examination of the specific associations reveals further insights. For F1, characterized by P_2O_5, SiO_2, and Ri, the negative loading of SiO_2 in conjunction with the positive loading of Ri suggests a reciprocal relationship; as SiO_2 concentrations increase, Ri may also rise correspondingly, indicating a potential balance between these variables. In F2, the strong negative loading associated with CaO implies an inverse correlation, indicating that elevated levels of CaO are linked to a reduction in the significance of this factor. Meanwhile, F3 demonstrates a robust association with both P_2O_5 and CaO, underscoring their potential interaction and co-occurrence in geological samples, which may reflect shared geochemical processes.

The fourth factor (F4) is notably associated with both MgO and CaO, suggesting that these oxides may derive from a common geochemical environment, further illuminating the intricacies of their interactions. Finally, F5 stands out due to its prominent positive loading for CO_2, indicating its unique role within the broader chemical context of this analysis.

5. Conclusion and Recommendations

The Djemi-Djema-Est phosphate deposit stands out as a critical resource for phosphate extraction in Algeria, supported by its advantageous geological structure and substantial reserves. This study underscores the unique characteristics of the deposit's Thanetian-age phosphate layer, which exhibits spatial variability in thickness influenced by natural irregularities and tectonic features. The absence of sterile intercalations and the extensive supra-layer coverage further enhance its viability for efficient mining operations.

Detailed mineralogical and petrographic analyses, particularly using XRD techniques, have identified the primary phosphatic phase as apatite group minerals. These are frequently associated with exogenous gangue materials, including carbonates, silica, and minor evaporitic phases such as gypsum. Geochemical assessments reveal the consistency of P_2O_5 content across the deposit, averaging 25.17%, while variations in MgO, SiO_2, and CaO contents provide valuable insights into the composition of the matrix and cement. These findings affirm the deposit's suitability for selective exploitation and efficient resource utilization.

To achieve sustainable management of this critical resource, addressing immediate operational challenges alongside broader resource stewardship considerations is imperative. Enhancing geological surveys is a priority. The proposed D1 survey aims to intersect the eastern fault mirror to quantify block offsets, improving understanding of structural complexities. The D2 vertical survey will validate the reported 8.5m phosphate thickness in central mining blocks, while the D3 survey focuses on delineating the pre-Miocene erosion surface to refine spatial models for selective exploitation.

Optimizing mining strategies is equally crucial for maximizing resource efficiency. Targeting areas with higher P_2O_5 content and favorable gangue-to-phosphate ratios will minimize waste extraction and enhance yield. Additionally, developing tailored beneficiation techniques to address site-specific mineralogical and geochemical variations, particularly reducing carbonate and silica impurities, will further improve operational efficiency.

Integrating sustainable practices into mining workflows is essential for minimizing environmental impacts. A long-term resource management plan should include comprehensive environmental impact assessments to ensure ecological preservation. Moreover, promoting the reuse of waste materials, such as dolomitic and calcareous gangue in construction or as soil amendments, can enhance sustainability efforts.

The broader significance of this study extends beyond the immediate mining context. The findings provide a foundation for guiding similar explorations in other parts of the Metlaoui-Gafsa-Onk transboundary basin. Collaborative efforts with regional and international stakeholders are necessary to align phosphate exploitation with global sustainable

development goals, particularly in agriculture and food security sectors. This study positions the Djemi-Djema-Est deposit as a model for efficient and environmentally responsible phosphate mining. The findings provide valuable insights that address the immediate needs of mining operations while highlighting the broader significance of integrating sustainable development principles. By adopting these principles, the industry can achieve long-term benefits that extend beyond resource extraction, fostering environmental stewardship and societal well-being. This research underscores the critical balance between operational efficiency and sustainable resource management, setting a benchmark for future phosphate mining projects.

Acknowledgments

This work was overseen by the IAWRSMB -Tunisia and the Laboratory of Applied Research in Engineering Geology, Geotechnics, Water Sciences, and Environment, Setif 1 University.

References

Abed, A. M., Arouri, K., Boreham, C. J. 2005. Source rock potential of the phosphorite bituminous chalk-marl sequence in Jordan. Marine and Petroleum Geology 22, 413-425.

Abou El Anwar, E., Abd El Rahim, S. 2022. Mineralogy, geochemistry and origin of the phosphorites at Um El Huwtat mine, Quseir, Central Eastern Desert, Egypt. Carbonates and Evaporites 37, 16.

Baioumy, H. M. 2007. Iron-phosphorus relationship in the iron and phosphorite ores of Egypt. Geochemistry 67(3), 229-239.

Barra, P. J., Pontigo, S., Delgado, M., Parra-Almuna, L., Duran, P., Valentine, A. J. 2019. Phosphobacteria inoculation enhances the benefit of P-fertilization on Lolium perenne in soils contrasting in P-availability. Soil Biology and Biochemistry 136, 107516.

Ben Hassen, A., Trichet, J., Disnar, J. R., Belayouni, H. 2011. Pétrographie et géochimie comparées des pellets phosphatés et de leur gangue dans le gisement phosphaté de Ras-Draâ (Tunisie). Implications sur la genèse des pellets phosphatés. Swiss Journal of Geosciences 103, 457-473.

Bezzi, N., Aïfa, T., Hamoudi, S., Merabet, D. 2012. Trace elements of Kef Es Sennoun natural phosphate (Jebel Onk, Algeria) and how they affect the various mineralurgic modes of treatment. Procedia Engineering 42, 1915-1927.

Boulemia, S., Adnet, S. 2023. A new Palaeogene elasmobranch fauna (Tebessa region, eastern Algeria) and the importance of Algerian-Tunisian phosphates for the North African fossil record. Annales de Paléontologie 109, 3, 102632.

Boulemia, S., Hamimed, M., Bouhlel, S., Bejaoui, J. 2015. Petro-mineralogical analysis of sedimentary phosphate of marine origin, case of the locality of El Kouif (Algerian-Tunisian confines). Open Journal of Geology 5(3), 156-173.

Boulemia, S., Hadji, R., Hamimed, M. 2021. Depositional environment of phosphorites in a semiarid climate region, case of El Kouif area (Algerian-Tunisian border). Carbonates and Evaporites 36(3), 1-15.

Boulemia, S., Hadji, R., Bouhlal, S., Hamed, Y., Besser, H., Ncibi, K. 2023. Geological and Mineralogical Analysis of Phosphorites in the Jebel Dhyr Syncline, Eastern Algerian Atlas. Mineralogia 54, 89-104.

Boumaza, B., Kechiched, R., Chekushina, T. V. 2021. Trace metal elements in phosphate rock wastes from the Djebel Onk mining area (Tébessa, eastern Algeria): a geochemical study and environmental implications. Applied Geochemistry 127,104910.

Bouzenzana, A. 2013. Harmful elements in concentrates of phosphate and method of disposal case of "Jebel-Onk" Algeria. The Journal of Ore Dressing 15, 25-30.

Chibani, A., Hadji, R., Younes, H. 2022. A combined field and automatic approach for lithological discrimination in semi-arid regions, the case of geological maps of Bir Later region and its vicinity, Nementcha mounts, Algeria. Geomatics, Landmanagement and Landscape 4.

Cielensky, S., Benchernine, N., Watkowski, T. 1988. Works of Prospecting and Assessment of Phosphates in the Region of Bir El Ater. In Internal Report. EREM (Entreprise de Recherche et d'Exploration Minière), Algeria, 103.

Cook, P. J., Shergold, J. H. 1984. Phosphorus, phosphorites and skeletal evolution at the Precambrian-Cambrian boundary. Nature 308, 231-236.

Cordell, D., White, S. 2011. Peak phosphorus: clarifying the key issues of a vigorous debate about long-term phosphorus security. Sustainability 3(10), 2027-2049.

Daneshgar, S., Callegari, A., Capodaglio, A. G., Vaccari, D. 2018. The Potential Phosphorus Crisis: Resource Conservation and Possible Escape Technologies: A Review. Resources 7(2), 37.

Dar Shamim, A., Khan, K. F., Birch, W. D. 2017. Sedimentary: Phosphates, Reference Module in Earth Systems and Environmental Sciences, Elsevier.

Dassamiour, M. 2012. Eléments en trace et valorisation des minerais de phosphates du gisement de Kef Essnoun, Jebel Onk (Algérie orientale). Unpublished Ph.D Thesis, Université Annaba, Algeria, 204.

Dassamiour, M., Mezghache, H., Raji, O., Bodinier, J. L. 2021. Depositional environment of the Kef Essennoun phosphorites (northeastern Algeria) as revealed by P_2O_5 modeling and sedimentary data. Arabian Journal of Geosciences 14, 1-17.

Desmidt, E., Ghyselbrecht, K., Zhang, Y., Pinoy, L., Van der Bruggen, B., Verstraete, W., Rabaey, K., Meesschaert, B. 2015. Global Phosphorus Scarcity and Full-Scale P-Recovery Techniques: A Review. Critical Reviews in Environmental Science and Technology 45, 336-384.

El Ayachi, M. S., Zagrarni, M. F., Snoussi, A., Bahrouni, N., Maher Gzam, M., Ben Assi, I., Hammami, K., Abdelli, H., Ben Rhaiem, H. 2016. The Paleocene-Lower Eocene series of the Gafsa basin (South-Central Tunisia): integrated stratigraphy and paleoenvironments. Arabian Journal of Geosciences 9, 35.

El Bamiki, R., Séranne, M., Chellaï, E. H., Merzeraud, G., Marzoqi, M., Melinte-Dobrinescu, M. C. 2020. The Moroccan High Atlas phosphate-rich sediments: Unraveling the accumulation and differentiation processes. Sedimentary Geology, 403, 105655.

El Bamiki, R., Raji, O., Ouabid, M., Elghali, A., Khadiri Yazami, O., Bodinier, J.-L. 2021. Phosphate Rocks: A Review of Sedimentary and Igneous Occurrences in Morocco. Minerals 11(10), 1137.

Ferhaoui, S., Kechiched, R., Bruguier, O., Sinisi, R., Kocsis, L., Mongelli, G., Bosch, D., Ameur-Zaimeche, O., Laouar, R. 2022. Rare earth elements plus yttrium (REY) in phosphorites from the Tébessa region (Eastern Algeria): Abundance, geochemical distribution through grain size fractions, and economic significance. Journal of Geochemical Exploration, 241, 107058.

Filippelli, G. M. 2011. Phosphate rock formation and marine phosphorus geochemistry: the deep time perspective. Chemosphere 84, 759-766.

Gadri, L., Hadji, R., Zahri, F., Benghazi, Z., Boumezbeur, A., Laid, B. M., Raïs, K. 2015. The quarries edges stability in opencast mines: a case study of the Jebel Onk phosphate mine, NE Algeria. Arabian Journal of Geosciences 8, 8987-8997.

Garnit, H., Bouhlel, S., Jarvis, I. 2017. Geochemistry and depositional environments of Paleocene-Eocene phosphorites: Metlaoui Group, Tunisia. Journal of African Earth Sciences 134, 704-736.

Hamdadou, M. 1996. Caractérisation pétro-minéralogique et séquentielle du gisement de phosphate de Jebel Onk (Algérie). Unpublished Ph.D. Thesis, Ecole Nationale Supérieure de Géologie de Nancy, France, 299.

Jaballi, F., Felhi, M., Khelifi, M., Fattah, N., Zayani, K., Abbes, N., Elouadi, B., Tlili, A. 2019. Mineralogical and geochemical behavior of heated natural carbonate apatite of the Ypresian series, Maknassy Mezzouna basin, central Tunisia. Carbonates and Evaporites 34, 1689-1702.

Kallel, A., Ksibi, M., Dhia, H., Khélifi, N. 2017. Recent advances in environmental science from the Euro-Mediterranean and surrounding regions. Proceedings of Euro-Mediterranean Conference for Environmental Integration (EMCEI-1), Tunisia 2017.

Kechiched, R. 2017. Phosphates from the north of Tébessa (Dyr and El-Kouif): sedimentological, gitological and geochemical study. Unpublished Ph.D. Thesis, Badji Mokhtar University, Annaba, Algeria, 225.

Kocsis, L., Ounis, A., Baumgartner, C., Pirkenseer, C., Harding, I. C., Adatte, T., Chaabani, F., Mohamed, S. 2014*a*. Paleocene-Eocene palaeoenvironmental conditions of the main phosphorite deposits (Chouabine Formation) in the Gafsa Basin, Tunisia. Journal of African Earth Sciences 100, 586-597.

Kocsis, L., Gheerbrant, E., Mouflih, M., Cappetta, H., Yans, J., Amaghzaz, M. 2014*b*. Comprehensive stable isotope investigation of marine biogenic apatite from the Late Cretaceous-Early Eocene phosphate series of Morocco. Palaeogeography, Palaeoclimatology, Palaeoecology 394, 74-88.

Lassis, M., Mizane, A., Dadda, N., Rehamnia, R. 2015. Dissolution of Jebel Onk phosphate ore using sulfuric acid. Environmental Nanotechnology, Monitoring and Management 4, 12-16.

Mahleb, A., Hadji, R., Zahri, F., Boudjellal, R., Chibani, A., Hamed, Y. 2022. Water-borne erosion estimation using the Revised Universal Soil Loss Equation (RUSLE) model over a semiarid watershed: Case study of Meskiana Catchment, Algerian-Tunisian Border. Geotechnical and Geological Engineering 40(8), 4217-4230.

Mezghache, H., Toubal, A., Bouima, T. 2004. Typology of phosphate ores of the Jebel Onk Mining Basin (Eastern Algeria). Phosphorus Research Bulletin 15, 5-20.

Nouioua, I., Fehdi, C., Boubaya, D., Serhane, B., Djellali, A. 2015. Mapping underground cracks using 2D electrical resistivity tomography: the case of the landslide of Kef Essenoun phosphate deposit, Djebel Onk (northeast of Algeria). Arabian Journal of Geosciences, 8(10), 7731-7738.

Ounis, A., Kocsis, L., Chaabani, F., Pfeifer, H. R. 2008. Rare earth elements and stable isotope geochemistry (δ13C and δ18O) of phosphorite deposits in the Gafsa Basin, Tunisia. Palaeogeography, Palaeoclimatology, Palaeoecology 268, 1-18.

Oussedik, M., Ousmer, N., Belkhedim, M. 1980. Phosphatic Eocene mineralizations in Algeria and the Jebel Onk phosphate deposit. Document of BRGM 24, 141-151.

Prian, G. P., Cortiel, P. 1993. Étude de développement du gisement de phosphate de Jebel Onk (Algérie). Unpublished Geological Expertise Report of BRGM, France, 288.

Pufahl, P. K., Groat, L. A. 2017. Sedimentary and igneous phosphate deposits: formation and exploration: an invited paper. Economic Geology 112, 483-516.

Strougo, A. 1976. Le groupe de Ostrea (Turkostrea) multicostata Deshayes. Géologie Méditerranéenne 3(1), 27-44.

Tahri, T., Bouzenzana, A., Bezzi, N. 2019. Characterization and homogenization of Bled El-Hadba phosphate ore, case of Jebel Onk (Algeria). Science Bulletin of the National Mining University 28, 35.

Tulsidas, H., Gabriel, S., Kiegiel, K., Haneklaus, N. 2019. Uranium resources in EU phosphate rock imports. Resources Policy 61, 151-156.

USGS - U.S. Geological Survey. 2020. Mineral commodity summaries 2020. U.S. Geological Survey, 200.

Wang, X.-Q., Ruan, W.-Y., Yi, K.-K. 2019. Internal phosphate starvation signaling and external phosphate availability have no obvious effect on the accumulation of cadmium in rice. Journal of Integrative Agriculture 18, 2153-2161.

Zerzour, O., Gadri, L., Hadji, R., Mebrouk, F., Hamed, Y. 2020. Semi-variograms and kriging techniques in iron ore reserve categorization: application at Jebel Wenza deposit. Arabian Journal of Geosciences 13(16), 820.

Zhang, Y., Li, Z., Dini, S. M., Qin, M., Banakhar, A. S., Li, Z., Yi, L., Memesh, A. M., Shammari, A. M., Li, G. 2021. Origin and evolution of the Late Cretaceous reworked phosphorite in the Sirhan-Turayf Basin, Northern Saudi Arabia. Minerals 11, 350.